

# Sprayed Metal Shells for Tooling: Improving the Mechanical Properties

P. S. Fussell<sup>†</sup>, Aluminum Company of America;  
H. O. K. Kirchner, Institut de Sciences des Matériaux, Université Paris-Sud;  
F. B. Prinz, Engineering Design Research Center, Carnegie Mellon University.

## Abstract

This work describes methods to improve the quality of the metal resulting from thermal spray deposition, including both the mechanical and metallurgical behavior. The engineering context is the production of sprayed metal shells suitable for tooling applications. The sprayed metal shells are mechanically dominated by interparticle interfaces; the particles are largely mechanically interlocked with very little metallurgical bonding. Based on these observations, improvements are made to these interfaces, and the measure of the improvement is shown in mechanical tests.

## Rapid Tooling and Sprayed Material

Rapid manufacturing of tooling for injection molding, stamping, composite lay-up, casting, or similar processes where the shape of the tool is critical presents a challenging problem possessing considerable commercial potential (Rothdeutsch 1990; Weiss, Gursoz et al. 1990). The tool, die, and fixture market amounted to about  $5 \times 10^9$  US\$ in 1989, and prototype to medium life tooling accounts for about 15% or  $750 \times 10^6$  US\$ of the total. The commercial literature reports the creation of such tooling by arc-spraying zinc and zinc alloys for at least 30 years (MOGUL 1963), and thick sprayed zinc structures have been in the literature for 68 years (Turner and Budgen 1926). Commercially viable, they save as much as 80% to 90% of the time required to make a prototype tool (two weeks for sprayed zinc versus twenty weeks for machined steel), and 75% of the cost (perhaps \$4,000 versus \$16,000). These alloy systems, however, are relatively soft and prone to wear and loading failure, which limits their usefulness to prototype tooling applications and low pressure applications such as reaction injection molding tooling.

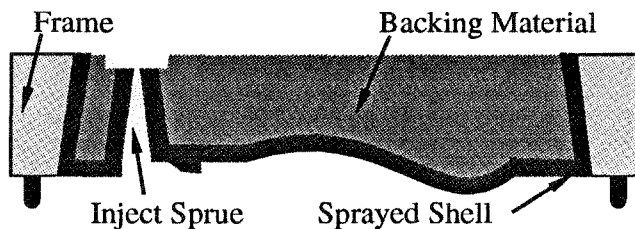


Figure 1. Schematic cross section of a sprayed tool; Angling the frame interior helps support compressive loads on the tool face.

Other possibilities for the materials of the tool face include aluminum bronze (Milovich 1989), which has much greater wear resistance compared to zinc systems. We describe the part and patterns needed to make the part's mold or die in a CAD system. A solid freeform fabrication process, stereolithography (Hull 1986; Hull 1990) in this case, autonomously creates the pattern in a matter of days. The shells are fabricated by spraying metal using an arc-spray device to create the tooling face and structure. Then, support material fills the back side of the tooling cavity to sustain the compressive service loads. Figure 1 shows a cross section of such a tool. For service at elevated temperatures ( $\sim 450$  °C); it is desirable to match the coefficients of thermal expansion of the sprayed tooling material and the backing material.

The basic fabrication of these sprayed ferrous tools had been described in (Fussell and Weiss 1990; Weiss and Schultz 1992; Weiss, Prinz et al. 1993). There are a number of concerns for a

<sup>†</sup> to whom correspondence should be addressed:

P. S. Fussell, Alcoa Technical Center, 100 Technical Drive, Alcoa Center, Pennsylvania 15069 USA

tool made in this way. After finishing the arc-spraying, the shell and the substrate still contain considerable internal stress, albeit in equilibrium (Gill and Clyne 1990; Gill 1991). The presence of internal stress in the shell, as well as a mismatch of coefficients of thermal expansion, raise questions of the shell's geometric stability at elevated temperatures, and over long times. Finally, the spray process is poorly suited for spraying into narrow channels and small aspect ratio holes.

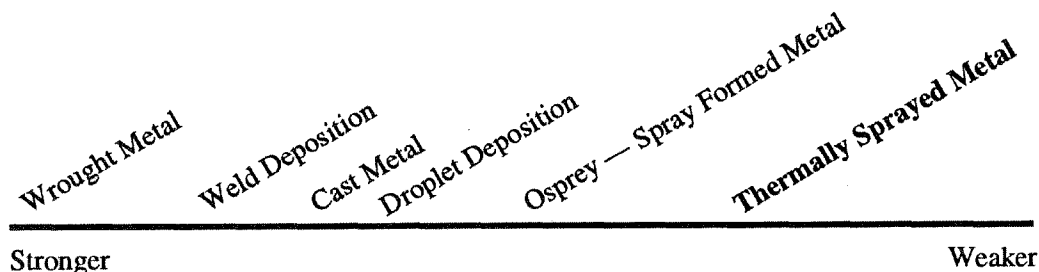


Figure 2. Generalized Continuum of **Material Strength**;  
(as-formed or as-cast materials).

Sprayed metal is chosen to provide the working surface of the tool for pragmatic reasons: once we have created the pattern's surface geometry, a complete working surface representing that geometry can be created in short order. On a generalized continuum of **material strength**, thermally sprayed metal, one of several alternatives, fits as shown in Figure 2. Poorly thermally sprayed metal has a tensile strength about 5% of wrought material of the same alloy. This is compared to 50% to 80% of normalized wrought materials for droplet deposited steel (Merz 1994).

However, Figure 3, another generalized continuum with respect to the **time** required to form complex geometries, highlights the economic interest in quickly forming complex shapes. The thermally sprayed material can quickly deliver a complex geometry.

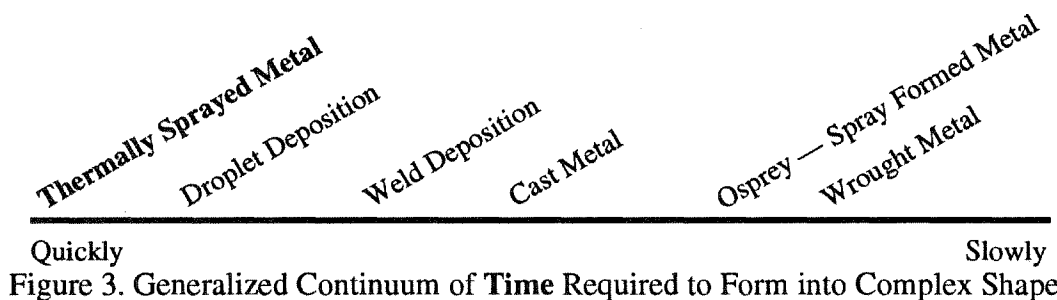


Figure 3. Generalized Continuum of **Time** Required to Form into Complex Shape.

In the same way that a tool's geometry determines much of its function, much of the tool's strength and wear characteristics are determined by the microstructure of the sprayed shell. The work described here is an attempt to find methods to locally, *i.e.*, microstructurally, improve the mechanical properties performance of the thermally sprayed metal. In short, the work here describes ways to move thermally sprayed ferrous and allied materials further up the continuum of strength displayed in Figure 2, while retaining the economic advantages created by speed of manufacture as shown in Figure 3. The methods explored here follow a path: reduce the oxide content, promote metallurgical bonding by permitting diffusion bonding to take place, and attempt to promote metallurgical bonding by adding superheat to the droplets that form the lamella of the shell.

One extremely interesting aspect of the sprayed tool work is its ability to build large tooling structures. Other newly developing rapid prototype systems suitable for manufacturing face the boundaries of either the volume of the tool they are building, or at the best by the surface area of the tool. Thus a doubling of tool volume can amount to an eight fold increase in production time.

The thermally sprayed tool, however, is bound by the area of the working surface. Scaling up from the current tooling experiments of 0.5 m by 0.5 m to tools requiring sizes of 2 m by 0.5 m will be an interesting and immediately addressable problem..

For perspective, other alternatives are being developed to quickly deliver a large prototype tool. The CMU effort to develop tooling structures by layered micro-casting deposition is extremely interesting (Merz, Prinz et al. 1994). The growing number of alternatives for fast production of investment cast tooling also draws attention, especially if someone invents a method for investment casting parts with an accuracy of the order of  $\pm 50 \mu\text{m}$  ( $\pm 0.002$  inches). Similarly, large cast tooling augers well, particularly for those tolerance regimes that accept accuracies of  $\pm 0.5 \text{ mm}$  ( $\pm 0.020$  inches). However, a leading competitor for this technological niche remains the more traditional CNC cutting of either the tool or the EDM electrodes used to burn the tool.

### Experimental Arrangements

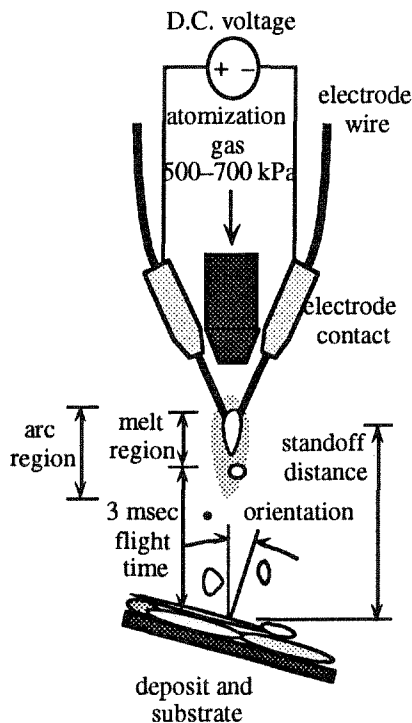


Figure 4. Schematic of an arc-spray gun and deposited particle flight times.

The effort reported here uses an arc-spray system (Cifuentes and Harris 1984; Thorpe 1989). The arc-spray gun is arranged as in Figure 4. Two consumable electrode wires are fed through contact tips to the area of the arc. A D.C. power supply establishes an arc between the wires, melting them in the arc. A column of atomizing gas, ranging from 480 kPa to 690 kPa (70 psi to 100 psi) ablates the molten material from the wires, atomizes the molten droplets and carries them, in a spray, to the substrate. For steel systems, the arc specific energy ranges from  $2.6 \text{ MJ Kg}^{-1}$  to  $3.0 \text{ MJ Kg}^{-1}$  giving a temperature of  $10^4 \text{ K}$  in the arc (Safai and Herman 1981). (Iron requires about  $700 \text{ kJ Kg}^{-1}$  energy to be melted from ambient temperature.) Deposition rates for an arc-spray system range from  $1 \text{ kg hr}^{-1}$  to  $20 \text{ kg hr}^{-1}$ .

Due to the large surface/volume ratio of the sprayed droplets, oxidation in flight and after impingement is a problem. The obvious way to circumvent the detrimental effect of oxidation and avoid the ensuing brittleness of the deposit is to minimize the partial pressure of oxygen in the gaseous atmosphere (Kaiser and Miller

Material	Sintering Temperature	Sintering Time
Fe-36Ni (INVAR)	1400 K (2075 °F)	30 min
Ni-5Al	1400 K (2075 °F)	30 min and 60 min
Fe-0.4C	1400 K (2075 °F)	30 min
50 vol % 308 Stainless & 50 vol % Copper	1170 K (1650 °F)	30 min
50 vol % 308 Stainless & 50 vol % 4043 Al	890 K (1150 °F)	30 min

Table 1. Sintering Schedule for Mechanical Properties Samples

1989). In these experiments, the partial pressure of oxygen was reduced by using a shroud arrangement around the spray region. The shroud gas was argon avoiding potential problems with nitride formation (Milewski and Sartowski 1986).

The samples for this experiment were uniformly sprayed onto a aggressively grit blasted mild steel coupon. After spraying, they were detached from the coupon, and then vacuum sintered with the intention of understanding what metallurgical bonding would develop and how that would affect the material performance. The sintering schedule, reminiscent of that for powder metallurgy sintering (Gall 1985), was as shown in Table 1. The temperature ramp up times from ambient to sintering temperature varied from 30 min to 1 hour. The vacuums were in the range of  $5 \times 10^{-6}$  to  $9 \times 10^{-6}$  bar.

### Improving the Properties

Figure 5 shows an SEM view of the sprayed material. This view is typical, and shows that the lamellæ are evidently not metallurgically bound together, or at least very seldomly and with only small cross section bridges (see arrows in Figure 5). In an effort to explore this condition, I mechanically tested the sprayed material in a number of conditions. Specifically:

- INVAR, as sprayed with air atomization (similar to that in Figure 5);
- INVAR, as sprayed in chamber (vacuum purged, backfilled to 0.5 Bar argon, and sprayed with argon atomization);
- INVAR, sprayed under argon shroud cover and then sintered for 30 minutes at 1400 K.
- 308 stainless steel, sprayed using the single wire plasma gun under argon shroud cover.

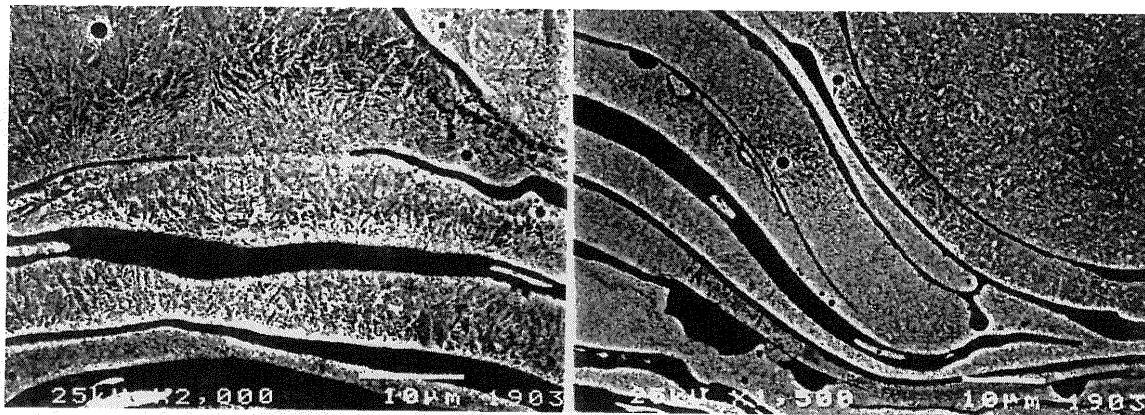


Figure 5. Mechanically linked thermally sprayed lamella.

The first test was the background measurement against which improvements were to be compared. This material is similar to that initially used in making tool shells. The second material was intended to remove the oxide from the material, but there is still substantial void porosity. The third experiment was done to see if the promotion of a diffusion bond would improve the material. The fourth test was to attempt to understand if it was possible to add enough superheat to the individual particles to promote bonding in the as sprayed condition, rather than adding the additional sintering step.

The material tests performed here are limited in scope. Given the nature of these microstructures, it is reasonable to assume that there will be a large measure of variability in the measurement data. I was interested in seeing general trends, rather than detailed statistically significant materials characterization. At best, shades of trends can be extracted from these data.

For the INVAR, the sintering conditions permitted a measure of metallurgical bonding to take place bringing the tensile strength up to nearly half of that expected from wrought material. More importantly, a meaningful amount of elongation has been recovered from the material. This will permit a tool made of such a material to locally adjust (deform) in response to inclusions or other stress risers.

Material	Condition	Tensile Strength	Elongation
Fe-36Ni (INVAR)	<i>for comparison, typical wrought mat'l</i>	500 MPa (75ksi)	30 %
Fe-36Ni (INVAR)	as sprayed, heavily oxidized	12 MPa (1.7 ksi)	0.14 %
Fe-36Ni (INVAR)	sprayed in chamber (Ar backfill, 0.5 Bar)	120 MPa (17 ksi)	0.23 %
Fe-36Ni (INVAR)	sprayed in shroud, sintered	<b>220 MPa (32 ksi)</b>	<b>2.8 %</b>
308 S.S.	<i>for comparison, typical wrought mat'l</i>	515 MPa (75ksi)	40%
308 S.S.	Sprayed with single wire plasma	<b>180 MPa (26 ksi)</b>	<b>0.3%</b>
Ni-5Al	sintered	<b>340 MPa (50 ksi)</b>	<b>4.5 %</b>

Table 2. Summary of Sprayed Material Mechanical Performance.

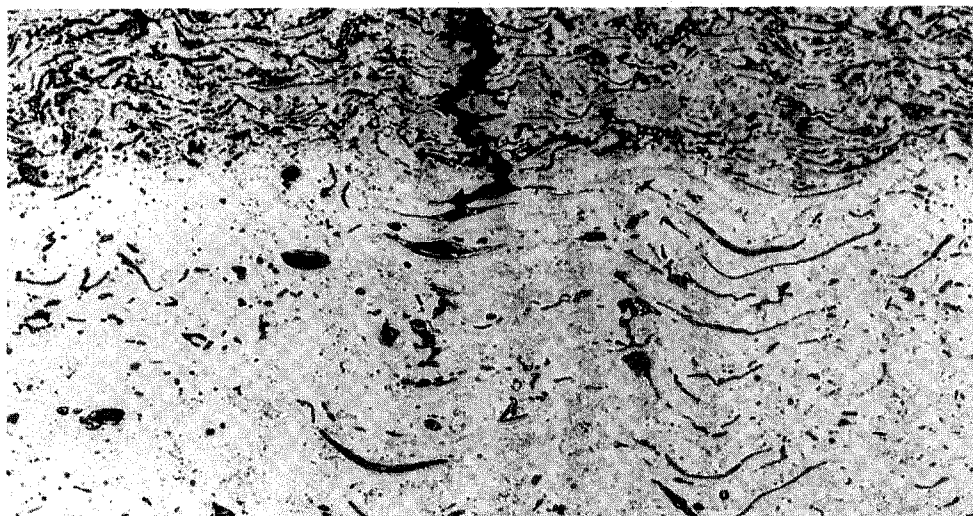


Figure 6. Crack propagation in sintered INVAR ending at the metallurgically bonded material.

The 308 S.S. material that was sprayed with the single wire gun shows considerable strength, but poor elongation. As will be seen in the fracture surface micrographs later on, the material seems to be failing in both the lamellæ regions and along inter-lamella boundaries, but the material is still essentially a rapidly solidified material and therefore it remains a relatively brittle substance.

Figure 6 provides a visual record of the mechanical improvement in an INVAR sample. The upper region of the sample is sprayed with unsatisfactory shielding, and therefore is laden with oxide. The lower region of the sample was sprayed with better inert shielding. The entire sample was sintered at 1400 K (2075 °F) for 30 minutes. The propagating crack was stopped by the metallurgically bonded lamellæ, even though there appears to be a relatively large amount of porosity and oxide still in the microstructure.

The fracture surfaces of the tested samples are illuminating. Figure 7 shows the same region in an Invar sample as Figure 6. This is the sample which was tested to tensile failure in Table 2, and the view is that of the fractured face of the specimen. The top area is the oxide dominated failure region, and the bottom area is the region where the lamellæ have metallurgically bonded. The top area is characterized by the relatively flat fracture surface — the crack was unimpeded by the lamellæ and proceeded along the weak and brittle oxide. However, the lamellæ in the lower portion of 7 clearly increased the difficulty of crack propagation: the surface has much more relief, and the lamellæ are clearly visible.

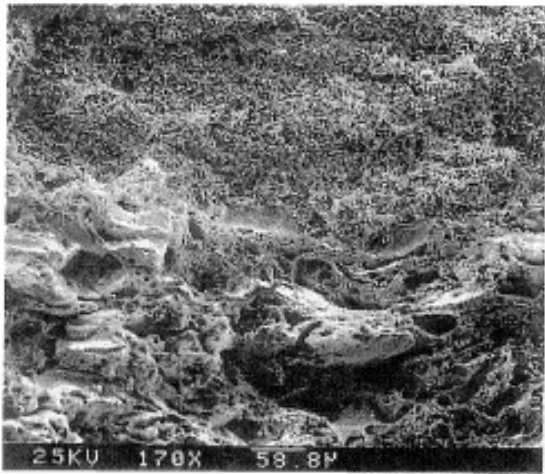


Figure 7. Sintered INVAR fracture surface. showing oxide dominated fracture (top) and bonded lamellæ dominated fracture (bottom).

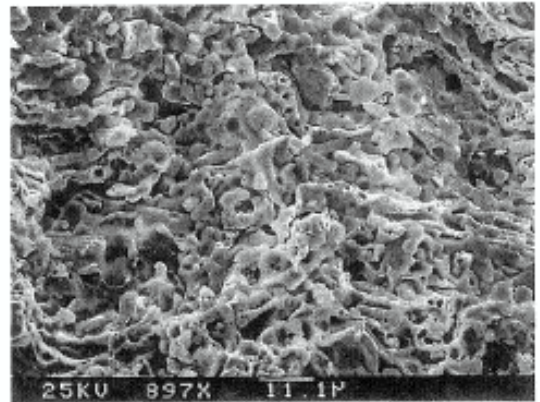


Figure 8. Sintered INVAR oxide fracture surface at higher magnification. (Showing oxide dominated region.)

Figure 8 shows in higher magnification the oxide dominated region of the fracture surface. Two aspects of the view in Figure 8 are noteworthy.

- The field of view is dominated by the small, sharp fractured oxide particles. These are the portion of the material that carried some load until failure and the failure crack propagated through their structure. Figure 8 shows why this oxide laden structure is fairly weak compared to our expectations for an oxide structure (which should be relatively strong if brittle) — the amount of oxide material carrying the load is a relatively small fraction of the total area of the cross section; there is a large fraction of void and the porosity doesn't contribute to the strength of the material.
- Underlying the crystalline fracture in Figure 8 is the relatively smooth surfaces of the undisturbed lamellæ. Where they are visible, there must have been a region of either void porosity or laminar porosity which opened during the fracture.

Figure 9 shows the companion pictures for the region in the sintered Invar where the failure was dominated by the lamellæ themselves. The magnification of 9 is similar to that of 8. Figure 9 shows the lamellæ which have either been cleaved in two, or the failure crack propagated along their boundary. I believe that both mechanisms are present: some of the lamellæ surfaces show characteristics of the wrought material fracture failure such as the graininess of the lamella surface and the small ridge-like surfaces on the lamella in the upper left region of 9. The material in 9 is still a rapidly solidified material that has been sintered for 30 minutes. There are also regions which appear to be boundary failures, particularly the small 15 µm by 20 µm lamella hole in the bottom center of 9. The dark cavern regions on the right side of 9 appear to be void porosity which has been exposed by the fracture.

The fracture face of the single wire plasma sprayed 308 stainless steel sample is shown in Figure 10. This material was sprayed with extra energy being provided to the plasma beyond that needed to melt the wire. The fracture surface shows several species of material condition. First, the lamellar structure is clearly visible in the layered organization of the metal. There are also some regions of apparent inter-laminar porosity visible in the structure. Secondly, there are several broken lamellæ, showing that the crack propagated through at least some of the lamellæ. All of the severed lamellæ in Figure 10 show signs of brittle fracture: there are chevrons on the visible faces. Thirdly, there are smooth lamellæ surfaces visible in the figure. These indicate that the crack was able to propagate along the inter-lamella boundaries in some areas. Notable is what is missing: the regular, crystalline structure of the oxide face is missing from these samples.

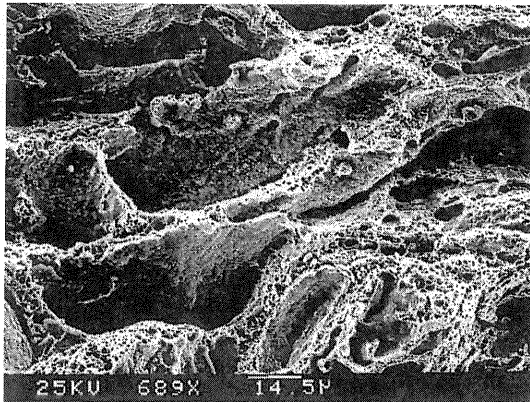


Figure 9. Sintered INVAR metallurgically bonded fracture surface showing fractured lamellæ and inter-lamella regions.

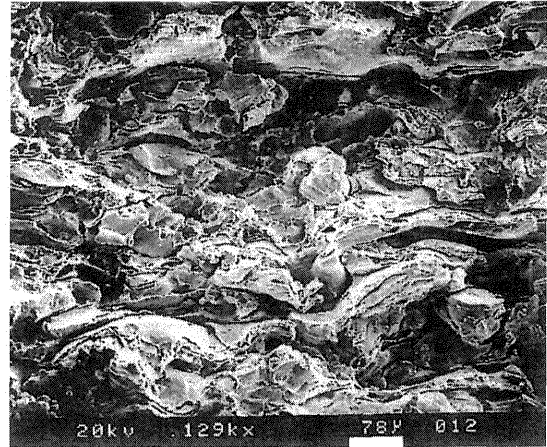


Figure 10. Single wire plasma sprayed 308 S.S. fracture surface, showing fractured lamellæ and inter-lamella regions.

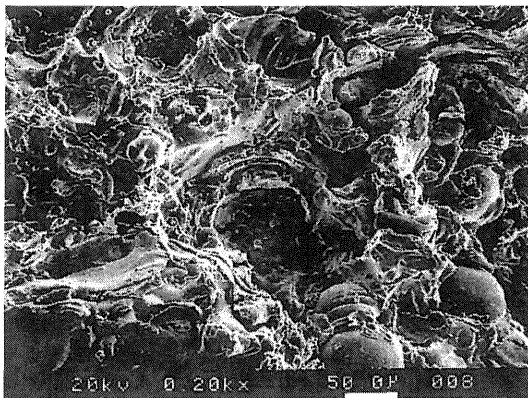


Figure 11. Detail: Single wire plasma sprayed 308 S.S. fracture surface, showing lamella pull-out, and fractured lamella regions.

Figure 11 is a slightly higher magnification micrograph of the same face of tensile tested 308 stainless steel. This picture clearly shows the spherical lamellæ that were formed by particles that solidified, or nearly solidified, in flight prior to impacting the shell. These particles did not, it appears in the figure, contribute to the strength of the shell. Rather, the failure crack propagated along their boundaries. In the center of Figure 11, there is a hole where a spherical lamella was pulled out from the face.

### Non-metallurgically Bonded Shells

The current art for making sprayed metal shells results in mechanically bonded lamellæ. A better shell can be made:

- Superheat in the particles will promote fusion with other lamellæ and lower the porosity of the shell — superheat is added to the particles by using a suitable energy source, by spraying with a heated gas stream, and by controlling the radiant heat loss;
- A hot substrate will largely eliminate quench stress, and help reduce porosity — the hot substrate is most easily provided by using a heat castable ceramic substrate;

- The sprayed particles should be of uniform size — the uniform size is a difficult challenge which can be met by a radically different deposition scheme such as the microcast method described in (Merz 1994), or by an extremely carefully managed spray atomizer;
- The partial pressure of oxygen must be minimized — the controlled atmosphere for the spray is easily delivered by a shroud arrangement, and might also be attained by a laminar flow inerting system such as that developed by Praxair or other commercial gas vendors.

Certainly the single-wire plasma device holds promise in delivering a number of these desiderata.

### Conclusions

The mechanical performance of thermally sprayed shells can be improved by promoting metallurgical bonding in the microstructure. However, the mechanisms for forming the bonds are defeated if each lamella is coated in an oxide. Further, if the void porosity fraction is too large, the strengths will not be significantly improved and the material will continue to exhibit a measure of anisotropy. Thus oxide control, process control to minimize void porosity, and a mechanism for metallurgical bonding are all simultaneously required to improve the mechanical performance. These microstructural issues will also be valid for other solid freeform fabrication methods which build up metal structures by an accumulation of individual particles.

### References

- Cifuentes, L. and Harris, S. (1984). "Composition and Microstructure of Arc-Sprayed 13% Cr Steel Coatings." *Thin Solid Films* 118(4): 515-526.
- Fussell, P. S., Patrick, E. P., Prinz, F. B., Schultz, L., Thuel, D. G., Weiss, L. E., Hartmann, K. W. and Kirchner, H. O. K. (1991). *A Sprayed Steel Tool for Permanent Mold Casting of Aluminum*. 1991 SAE Aerospace Atlantic, Dayton, Ohio USA, SAE International.
- Fussell, P. S. and Weiss, L. E. (1990). *Steel-Based Sprayed Metal Tooling*. Solid Freeform Fabrication Symposium, Austin, Texas USA, University of Texas — Austin.
- Gall, H. E. B. a. T. L., Ed. (1985). *Metals Handbook Desk Edition*. Metals Park, Ohio, ASM.
- Gill, S. C. (1991). *Residual Stresses in Plasma Sprayed Deposits*. Ph. D. University of Cambridge, England
- Gill, S. C. and Clyne, T. W. (1990). "Stress Distributions and Material Response in Thermal Spraying of Metallic and Ceramic Deposits." *Metallurgical Transactions B* 21B: 377-385.
- Hull, C. W., I. UVP. US Patent 4,575,330 B1. Apparatus for Production of Three-Dimensional Objects by Stereolithography. Dec. 19, 1989.
- Hull, C. W., I. 3D Systems. US Patent 4,929,402. Method for Production of Three-Dimensional Objects by Stereolithography. May 29, 1990.
- Kaiser, J. J. and Miller, R. A. (1989). "Inert Gas Improves Arc-Sprayed Coatings." *Advanced Materials and Processes* 136(6): 37-40.
- Merz, R. (1994). *Shape Deposition Manufacturing*. Dissertation., Technische Universität Wien, Institut für Allgemeine Elektrotechnik und Elektronik
- Merz, R., Prinz, F. B. and Weiss, L. E., C. M. University. US 5,281,789. Method and Apparatus for Depositing Molten Metal. Jan 25, 1994.
- Milewski, W. and Sartowski, M. (1986). Some Properties of Coatings Arc-Sprayed in Nitrogen or Argon Atmosphere. *Advances in Thermal Spraying*. Oxford, Pergamon Press. 467-473.
- Milovich, D. (1989). *Metal-Faced Composite Tooling*. Tooling for Composites, Long Beach, California, SME.
- MOGUL (1963). *Metallizing Manual*. Metallizing Company of America.
- Rothdeutsch, J. G. a. E. (1990). *Rapid Tool Manufacturing — Commercial Investigation*.
- Safai, S. and Herman, H. (1981). Plasma-Sprayed Materials. *Treatise on Materials Science and Technology*. Academic Press. 183-214.
- Thorpe, M. L. (1989). *How Recent Advances in Arc Spray Technology have Broadened the Ranges of Applications*. Thermal Spray Technology: New Ideas and Processes, Cincinnati, Ohio USA, ASM International.
- Turner, T. H. and Budgen, N. F. (1926). Metal Spraying. *Metal Spraying*. London, Charles Griffin & Co. 162.
- Weiss, L. E., Gursoz, E. L., Prinz, F. B., Fussell, P. S., Mahalingam, S. and Patrick, E. P. (1990). "A Rapid Tool Manufacturing System Based on Stereolithography and Thermal Spraying." *Manufacturing Review* 3(1): 40-48.
- Weiss, L. E., Prinz, F. B. and Gursoz, E. L., C. M. University. US Patent 5,189,781. Rapid Tool Manufacture. Mar 2, 1993.
- Weiss, L. E. and Schultz, L. L., C. M. University. US Patent 5,079,974. Sprayed Metal Dies. January 14, 1992.